Atomic observation of structural evolution of turning aluminum surface during ion beam bombardment

Chunyang Du[1,2,3,#], Tao Lai[1,2,3], Xiaoqiang Peng[1,2,3], Shanyong Chen[1,2,3] and Cheng Huang[1,2,3]

1 College of Intelligence Science, National University of Defense Technology, Changsha 410073, China
2 Laboratory of Science and Technology on Integrated Logistics Support, National University of Defense Technology, Changsha 410073, China
3 Hu'nan Key Laboratory of Ultra-precision Machining Technology, Changsha 410073, China
Corresponding Author / Email: nature_cydu@vip.sina.com

KEYWORDS: Aluminum, Ion beam bombardment, Structural evolution, Molecular dynamics

Revealing structural evolution of turning aluminum surface during ion beam bombardment will benefit the optical surface quality modulation of aluminum, which is significant but challenging. In this paper, we present a molecular dynamics study on structural evolution and atom diffusion during ion beam bombardment. Metamorphic layer will generate during single point diamond turning causing massive sub-surface defects, which increases with the turning depth. During ion beam bombardment, the defects will perish with cascade collision. Thus, local stress will be released. Atom diffusion will be blocked by subsurface defects, which will decrease the degree of cascade collision. The whole surface presents a more stable state, which will benefit the surface roughness control during ion beam bombardment, thereby inducing a better finishing surface quality. The work gives an atomic-level insight into the structural evolution of turning aluminum surface during ion beam bombardment. The results provide guidance for the application of ion beam bombardment in the fabrication of high-surface quality of aluminum optics.

1. Introduction

Aluminum has attracted the interest of scientific and engineering communities, because of its outstanding mechanical and optical properties [1-3]. Aluminum is an ideal material for aerospace optical imaging system. With the application spectrum improving to visible (VIS) light, the imaging system requires nanoscale machining precision for the aluminum optical surface, which is hardly acquired by commonly used processing method such as Single point diamond turning (SPDT) and Magnetorheological finishing (MRF). Based on physical sputtering effect, ion beam sputtering (IBS) can achieve nanoscale material removal [4,5], which is recognized as the highest precision machining technique and has great potential improving machining precision of aluminum optical surface [6,7]. However, the turning aluminum surface induces severe heterogeneous characteristics, causing unique micromorphology evolution and even surface roughness deterioration [8]. IBS is often used as the final process in nano/sub-nanometer precision machining processes, which requires micromorphology manipulation and surface roughness control. Thus, it is crucial to understand the machining mechanism of aluminum during IBS.

The micromorphology evolution during IBS is highly concerned by many researchers recently [9-11]. Up to now, the studies of amorphous materials such as fused silica and monocrystalline silicon are very thorough. However, the research on polycrystalline materials such as polycrystalline Al is still lacking. The surface evolution and material removal during IBS occur at nanoscale time and space, which are hard characterized by experimental methods. Peculiar relief and gravel morphology of aluminum surface observed in the process of ion beam sputtering experiment cannot be explained by previous theory [12]. Molecular dynamics (MD) method has been widely used in revealing the interaction between energy particle and matrix [13–15]. Hence, it is feasible to reveal the surface evolution and material removal mechanisms during the IBS of aluminum optical surface via MD simulation. Although surface modification and structure evolution of aluminum under argon ion bombardment has been reported [16], the polycrystalline effect has not been considered and revealed. An in-depth study on the process and mechanism of ion beam machining on aluminum optical surface is significant yet challenging.

In the present work, the machining mechanism of aluminum optical surface during ion beam sputtering are explored via molecular dynamics simulation. In section 2, the model and method are presented. In section 3, metamorphic layer analysis and the evolution of surface morphology are discussed. Finally, the conclusions are drawn in section 4. The results provide the atomic-level insight into the IBS process of aluminum optical surface. The mechanism and regularity

lay a theoretical foundation for the application of IBS in the machining field of lightweight polycrystalline metal materials to achieve high-precision optical surface.

2. 2. Model and method

2.1 molecular simulation model

Fig. 1 shows the MD simulation model of SPDT of polycrystalline aluminum. The model contains a polycrystalline aluminum workpiece and a rigid diamond cutting tools. Table 1 presents the computational parameters used in the MD simulations. The size of the workpiece is 32nm × 32nm × 32nm, which contains 8 grains. The rake angle, relief angle and tool edge radius of turning tools 0°, 11° and 30nm, respectively. The edge radius is 1.5nm. The tool is treated as a rigid body in the simulation.

Table 1. SPDT computational parameters of MD simulation

Materails	Workpiece: polycrystalline aluminum
	Tool: daimond
Dimension	Workpiece: 32nm x 32nm x 32nm
	Tool: rake angle 0°; relief angle 11°; tool edge radius 30nm; edge radius 1.5nm
Number of atoms	2554949
Time step	1fs
Initial temperature	293k
Turning velocity	5m/s
Depth of cut	0.6nm; 1.2nm; 1.8nm; 2.4nm
Cutting distance	24nm

The workpiece includes three types of atoms: boundary atoms, thermostat atoms and Newtonian atoms. The motions of the thermostat and Newtonian atoms obey the classical second Newton's law. The equations of motion will be numerically integrated by Velocity-Verlet algorithm with the time step of 1fs. Boundary atoms locate on the left and bottom of the workpiece, which are fixed to eliminate the rigid body motion. The thermostat atoms adjacent to the boundary atoms. The initial temperature of workpiece is 293K. A periodic boundary condition is adopted along the y direction. Two different atomic potentials are applied on the simulation: (1) the interaction between Al atoms (Al-Al) is described by embedded atom method (EAM) potential; (2) the interaction between workpiece and tool (Al-C) is described by the Morse potential. The cur-off radius of the Morse potential is chosen to be 0.9025nm.

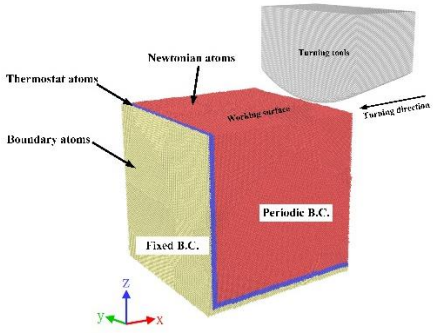

Fig. 1 MD simulation model of SPDT of polycrystalline aluminum.

After SPDT, the workpiece is used for IBF process. The computational parameters are presented in Table 2. The Ar ions are placed at the height of 2nm above the sample initial top surface. Considering the commonly used process parameters of IBF, the ion energy is chosen to be 500eV and the incident angle is 90°, as shown in Fig. 2. The sputtering area is the turned surface. Ziegler-Biersack-Littmark (ZBL) potential is adopted for Ar-Ar atomic interaction. For Al-Al atomic interaction, the embedded-atom method (EAM) potential is adopted. For Al-Ar atomic interaction, splicing potentials combined with ZBL, the second order polynomial function and Lennard-Jones (LJ) potentials are used.

Table 2. IBF computational parameters of MD simulation

Time step	1fs
Incident angle	90°
Ion energy	500eV
Ion number	50
Ion dose	$2.2*10^{13}$ ion/cm^2

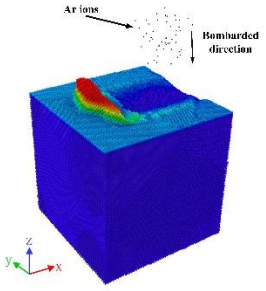

Fig. 2 MD simulation model of IBF of polycrystalline aluminum.

3. MD simulation and results

3.1 Metamorphic layer analysis

After relaxation of 1200ps, all atoms are in a minimal potential energy state. Comparing with the initial model, the width of grain boundaries increases and the shape of grain boundary changes from straight line into irregular curve. Atoms in grain boundaries vary from Other to HCP or BCC atoms. The FCC atoms are eliminated by Common neighbor analysis (CNA) to address the variation of other atoms. Fig. 3 presents the evolution of internal defects with different cutting distance. When the cutting hasn't start, the defects are distributed in the grain boundaries due to the relaxation process. When the cutting begins, a few stacking fault nucleate and expand from the grain boundaries, as shown in Fig. 3(b). When the cutting depth is 17nm, stacking faults are generated inside of the grains. Most of stacking faults are concentrated on the grains that interacts directly with the tool. But some stacking faults nucleate and verge to expand to the next grains due to material extrusion. With increase of cutting distance, the number of stacking faults in the next grains increases due to the destruction of grain boundary, as shown in Fig. 4(d).

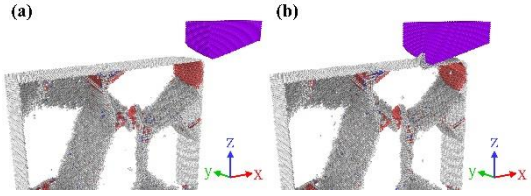

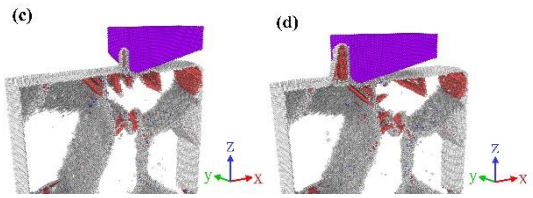

Fig. 3 Defect structure variation under cutting depth of 0.6nm with cutting distance of, (a) 0nm, (b) 11nm, (c) 17nm, (d) 24nm.

Fig. 4 shows metamorphic layer distribution with different cutting depth. A higher cutting depth causes more material extrusion and the lattice structures beneath the tool are subjected to more deformation effect. Moreover, with higher cutting depth, the grain boundary damage is more severe, as shown in Fig. 4(d)(h), and the rearrangement of atoms is more difficult, leading to more amorphous structure, such as dislocation cores. Thus, the depth and amount of the stacking faults increase with the cutting depth as well as the metamorphic layer.

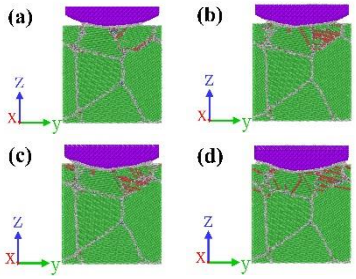

Fig. 4 The view of stacking faults and metamorphic layer distribution along *yoz* with cutting depth of, (a) 0.6nm, (b) 1.2nm, (c) 1.8nm, (d) 2.4nm.

3.2 IBS analysis

Ion sputtering simulation was carried out on the surface after turning. Fig. 5 shows the surface morphologies after turning and ion sputtering at different turning depths. For the surface morphology after turning, the tool is clearly turned (higher on both sides). Because the turning depth is small, the change of surface morphology is not obvious for all the turning surfaces. After ion sputtering, the surface quality deteriorated significantly, and the surface did not have obvious polycrystalline characteristics due to the destruction of grain boundaries. However, for the workpiece with different turning depth, the surface morphology after ion sputtering is obviously different. With the increase of the workpiece turning depth, the surface after ion sputtering is smoother and the surface quality is relatively better.

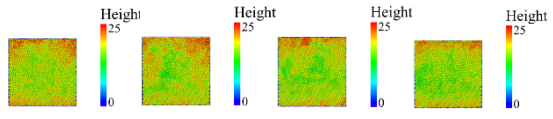

(a)0.6nm (b)1.2nm (c)1.8nm (d)2.4nm

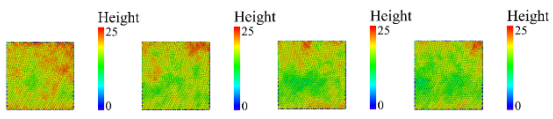

(e)0.6nm (f)1.2nm (g)1.8nm (h)2.4nm

Fig. 5 surface morphology of turning surface and sputtering surface with turning depth of, (a) 0nm, (b) 11nm, (c) 17nm, (d) 24nm.

The surface roughness of the workpiece with different turning depths was statistically analyzed. The surface roughness of the workpiece with turning depth of 0.6nm, 1.2nm, 1.8nm and 2.4nm was 1.3264A, 1.3462A, 1.4415A and 1.5034A, respectively. With the increase of turning depth, its roughness has a slight increase, this is because under the large turning amount, the deformation and rebound of the material will be more obvious, but because the cutting amount is at a small level, the roughness difference is relatively small. After ion sputtering, the surface roughness is 2.127 A, 1.906A, 1.8247 A and 1.7085 A, respectively. The roughness results also support the surface topography results in Fig. 5 (e)~(h). Combined with the results of turning roughness, the deterioration of surface quality of the workpiece with deeper cutting depth is less obvious. This is due to the larger amount of workpiece turning, the degree of sub-surface damage is more serious, preventing further perturbation of atoms to reduce the deterioration of surface quality.

4. Conclusions

Enabled by MD simulation, the process and mechanism of ion beam machining on aluminum optical surface were studied from the atomic level.

(1) The formation mechanism of turned metamorphic layer in ultra-precision single point diamond turning and its influence on ion beam machining were revealed. Based on the study of molecular dynamics, due to the destruction of grain boundaries and the formation of many dislocations, a turning metamorphic layer composed of amorphous layer and polycrystalline damaged layer will be formed on the surface after turning. Due to the destruction of grain boundaries, the surface material properties tend to be consistent, and the appearance of damage will hinder the atomic disturbance during the bombardment process, which will slow down the deterioration of the surface quality. When the metamorphic layer is completely removed and the bombardment depth reaches the intrinsic surface of the matrix, the relief structure will dominate the evolution process of the surface micro-light morphology.

(2) The mapping between the thickness of the turning metamorphic layer and the processing parameters is obtained, and the optimization direction is proposed according to the actual processing conditions. The increase of the thickness of turning metamorphic layer will help to slow down the deterioration rate of surface quality during ion beam processing of aluminum alloy reflectors. The optimization of turning parameters will be conducive to the increase of the thickness of the turned metamorphism layer. In the process of ultra-precision turning, the optimization space of turning speed and feed rate is small, so the main optimization parameter is determined to be the turning depth. Based on the molecular dynamics study, the thickness and number of dislocations of the turned metamorphic layer increase significantly with the increase of the turning depth, and the surface roughness of the generated surface is obviously lower after ion beam sputtering.

The work gives an atomic-level insight into the surface characteristic evolution and material removal mechanism during the

IBS of turning Al. The results provide guidance for the application of IBS in the machining of high-surface quality polycrystalline metal materials with nanoscale precision.

ACKNOWLEDGEMENT

This research was funded by Major Programs of the National Natural Science Foundation of China (Grant No.51991371), the National Natural Science Foundation of China (Grant No.51835013) and Foundation of State Key Lab of Digital Manufacturing Equipment & Technology (Grant No.DMETKF2022006)

REFERENCES

1. Bauer A, Rolland JP. “Visual space assessment of two all-reflective, freeform, optical see-through head-worn displays,” Opt Express., 22:13155-13163, 2014.

2. Wang Y, Li Z, Liu X, Fang F. “Freeform-objective Chernin multipass cell: application of a freeform surface on assembly simplification,” Appl Optics, 56:8541-8546, 2017.

3. Wamboldt L, Roy B, Crifasi J, Stephens S, Hanninen D, Woodard K, Felock R, Polczwartek S, Parenteau J. “An ultra-low surface finish process for 6061-Al mirrors,” Proc Of SPIE., 9451:94511X1-94511X9, 2015.

4. Weiser M. “Ion beam figuring for lithography optics,” Nucl Instrum Meth B., 267:1390-1393, 2009.

5. Frost F, Fechner R, Ziberi B, Vollner J, Flamm D, Schindler A., “Large area smoothing of surfaces by ion bombardment: fundamentals and applications,” J Phys Condens Matter., 21:224026, 2009.

6. Fang Z, Zhang Y, Li R, Liang Y, Deng H., “An efficient approach for atomic-scale polishing of single-crystal silicon via plasma-based atom-selective etching,” Int J Mach Tool Manuf., 159:103649, 2020.

7. Zhou G, Bi Y, Ma Y, Wang L, Wang X, Yu Y, Mutzke A., “Large current ion beam polishing and characterization of mechanically finished titanium alloy (Ti6Al4V) surface,” Appl Surf Sci., 476:905–913, 2019.

8. Bauer J, Frost F, Arnold T. “Reactive ion beam figuring of optical aluminum surfaces,” J Phys D: Appl Phys., 50:085101, 2017.

9. Keller A, Facsko S, Moller W. “Evolution of ion-induced ripple patterns on SiO2 surfaces,” Nucl Instrum Meth B., 267:656-659, 2009.

10. Xu MJ, Dai YF, Zhou L, Peng XQ, Chen SS, Liao WL. “Evolution mechanism of surface roughness during ion beam sputtering of fused silica,” Appl Opt., 57:5566-5573, 2018.

11. Chkhalo NI, Churin SA, Mikhaylenko MS, Pestov AE, Polkovnikov VN, Salashchenko NN, Zorina MV. “Ion-beam polishing of fused silica substrates for imaging soft x-ray and extreme ultraviolet optics,” Appl Opt., 55:1249-1256, 2016.

12. Du CY, Dai YF, Hu H, Guan CL. “Surface roughness evolution mechanism of the optical aluminum 6061 alloy during low energy Ar+ ion beam sputtering,” Opt Express., 28:34054-34068, 2020.

13. Papanikolaou M, Salonitis K. Fractal. “Roughness effects on nanoscale grinding.” Appl Surf Sci., 467:309–319, 2019.

14. Liu B, Xu Z, Wang Y, Gao X, Kong R. “Effect of ion implantation on material removal mechanism of 6H-SiC in nano-cutting: A molecular dynamics study,” Comp Mater Sci., 174:109476, 2020.

15. Feng H, Cui SY, Chen HT, Song XH, Fang QH, Li J, Liu B, Liu F. “A molecular dynamics investigation into deformation mechanism of nanotwinned Cu/high entropy alloy FeCoCrNi nanolaminates.” Surf Coat Technol., 401:126325, 2020.

16. Niu CN, Han JY, Hu SP, Song XG, Long WM, Liu D, Wang GD. “Surface modification and structure evolution of aluminum under argon ion bombardment,” Appl Surf Sci., 536:147819, 2021.